International Journal of Engineering Innovation & Research
Volume 4, Issue 5, ISSN: 2277 – 5668

Magnetic Characterization of Amorphous/ Nanostructured Phase Evolved in $Fe_{73.5}Cu_1Mo_{1.5}V_{1.5}Si_{13.5}B_9$

S. M. A. Rahim
Department of Applied Physics, Electronics and Communication Engineering, Islamic University, Kushtia

S. Manjura Hoque
Materials Science Division, Atomic Energy Centre, Dhaka, Bangladesh

M. M. Haque
Department of Applied Physics, Electronics and Communication Engineering, Islamic University, Kushtia

S. Akhter
Atomic Energy Centre, Dhaka

***Abstract* – The rapidly quenched $Fe_{73.5}Cu_1Mo_{1.5}V_{1.5}Si_{13.5}B_9$ alloy has been melt-spun to form ribbons where the refractory element of Nb has been replaced by equiatomic ratio of Mo and V in order to study the effect of these refractory elements on the magnetic properties. The ribbons have been annealed in a controlled way in the temperature range of 300°C to 600°C for 30 minutes in order to study its effect on structural parameters. DTA curve is characterized by the presence of α-Fe(Si) phase in the range of 458°C < T_a< 545°C and iron boride phase for T_a> 586°C. The activation energy of crystallization of α-Fe(Si) and Fe-B phase has been obtained as 2.80 and 4.18 eV respectively by using DTA. Enhanced value of initial permeability by two orders of magnitude and very low value of relative loss factor of the order of 10^{-5} has been observed with the variation of annealing temperature, which shows that Fe-based alloys of this composition with the simultaneous presence of Mo and V instead of Nb also bears ultra-soft magnetic properties. Increase of magnetization in the amorphous relaxed state is associated with structural relaxation. In the nanocrystalline state magnetization decreases because relative amount of Fe in the α-Fe(Si) nanograins decreases and relative amount of non-magnetic Mo, V and B in the amorphous matrix increases.**

***Keywords* – Initial Permeability, Relative Loss Factor, Saturation Magnetization, Bohr Magneton, Iron Silicon, X-Ray Diffraction.**

I. INTRODUCTION

Nanocrystalline materials represent one of the most active research items in recent times for the tailoring of materials with specific properties and property combinations. However, it is still in its infancy since its emergence as a major materials science has just begun at this stage of development. There have been glimpses of exciting new properties like super plasticity, giant magneto-resistance (GMR), transparency in opaque ceramics, enhanced homogeneity, unusual soft ferromagnetic and giant magneto-caloric effects, possessed by material which has been reduced to nanometer dimension.

Ultra-soft magnetic properties of Fe-rich FINEMET type of alloy has been brought under intense study due to its novel properties [1-5] since controlled crystallization from the amorphous state seems to be a very effective method presently available to synthesize nanocrystalline alloys with attractive soft magnetic properties. The amorphous nanocrystalline ribbons prepared by rapid solidification from the melt are in a metastable state and tend to transform into stable crystalline phases. The three kinds of stability for amorphous magnetic alloys are: resistance to the initiation of crystallization, structural relaxation effects and the relaxation or reorientation of directional order. At temperature below the crystallization temperature, structural relaxation effects take place and are caused by atomic rearrangements. From the thermodynamic view point [6] [7], the ability of an alloy to be quenched into the glassy state is generally measured by the magnitude of the quantity,

$$\Delta T_g = T_m - T_g, \quad (2.1)$$

Where T_m and T_g are the melting and glass transition temperatures respectively. In a similar manner the stability of the glass after formation is generally measured by the magnitude of the quantity,

$$\Delta T_x = T_x - T_g, \quad (2.2)$$

Where T_x is the temperature for the onset of crystallization.

The crystallization is associated with nucleation and growth process. The formation of an amorphous alloy depends on the absence of long-range order therefore change of composition is expected to affect T_g and T_x. In this experiment, crystallization temperatures were determined by differential thermal analysis and accordingly annealed at different temperatures. The attempt was to study the effect of grain size on magnetic permeability and saturation magnetization upon evolution of nanograins of different sizes with varying annealing temperatures. The composition has been selected as $Fe_{73.5}Cu_1Mo_{1.5}V_{1.5}Si_{13.5}B_9$, where equiatomic ratio of the refractory elements, Mo and V has been employed to act as grain growth inhibiter.

II. EXPERIMENTAL

Amorphous alloys in the form of ribbons have been prepared with the nominal composition $Fe_{73.5}Mo_{1.5}V_{1.5}Si_{13.5}B_9$ by single roller melt-spinning technique in air. The ribbons are on an average 6 mm wide and 20-25 □ m thick. The amorphosity of the ribbons has been confirmed by

PW 3040 - X″Pert Pro (Philips) X-ray diffractometer with Cu K□ radiation. X-ray diffraction studies have also been performed on samples annealed at different temperatures. The grain size and the composition of the nanograins are estimated from X-ray diffraction results by using full width at half maximum (FWHM) and peak shift. Temperature dependence of initial permeability of the as-cast ribbons are measured using a laboratory built furnace and Wayne Kerr 3255 B impedance analyzer with continuous heating rate of 5°C/min with very low applied ac field of ≈ 10^{-3} Oe. From this measurement, Curie temperature, T_c, of the as-cast amorphous phase has been determined. Frequency dependence of complex initial permeability of the amorphous and the annealed samples were measured in the frequency range of 1-500 kHz. Room temperature magnetization has been carried out by vibrating sample magnetometer.

III. Results and Discussion

Kinetics of crystallization of different crystalline phases has been studied by using differential thermal analysis. DTA diagrams of $Fe_{73.5}Cu_1Mo_{1.5}V_{1.5}Si_{13.5}B_9$ amorphous ribbon measured in nitrogen atmosphere with continuous heating rate of 10°C-40°C/min at step of 10°C is shown in Figure 1.

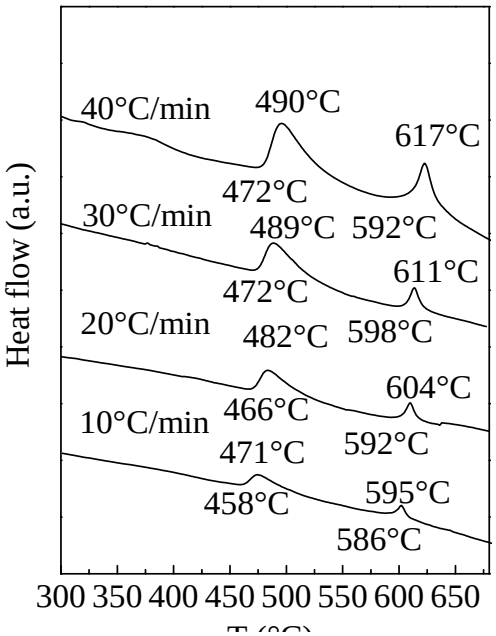

Fig.1. DTA curves of as-cast sample of $Fe_{73.5}Cu_1Mo_{1.5}V_{1.5}Si_{13.5}B_9$ alloy at different heating rate 10 – 40°C/min.

In Figure 1, two exothermic peaks in the curve indicate two distinct crystallization temperatures, the first one corresponds to the crystallization of α-Fe(Si) phase and the second one is related to the crystallization of iron boride. Mo and V act as grain growth inhibiter, which delays the crystallization of α-Fe(Si) and Fe-B phase and there is a wide temperature difference between two crystallization phases. Due to less miscibility of Cu in Fe-based alloy and small amount of Mo and V in the present sample, crystallization of Fe(Si) and Fe-B phases take place within wide temperature range, which facilitates to tailor its properties by controlling the volume fraction of different phases. For the heating rate of 10°C/min, the initiation of crystallization is around 458°C and the process of crystallization is completed at 489°C while the peak temperature is 471°C. This indicates that no crystalline phase is formed below 458°C and the crystallization process is completed within a wide range of temperature. From the figure, it is observed that the peak temperature shifts to higher values with the increase of heating rate.

The activation energy of crystallization of α-Fe(Si) and iron boride phases have been evaluated using Kissinger's plot of $\ln\frac{\beta}{T_p^2}$ versus $\frac{1}{T_p}$ presented in Figure 2 and 3, where β is the heating rate (10- 40°C/min. in this experiment) and T_p is the peak temperature of α-Fe(Si) and iron boride phases for each of the heating rate. Activation energy of crystallization of α-Fe(Si) and iron boride phases have been evaluated using Kissinger's plots and found to be 2.80 eV and 4.18 eV respectively.

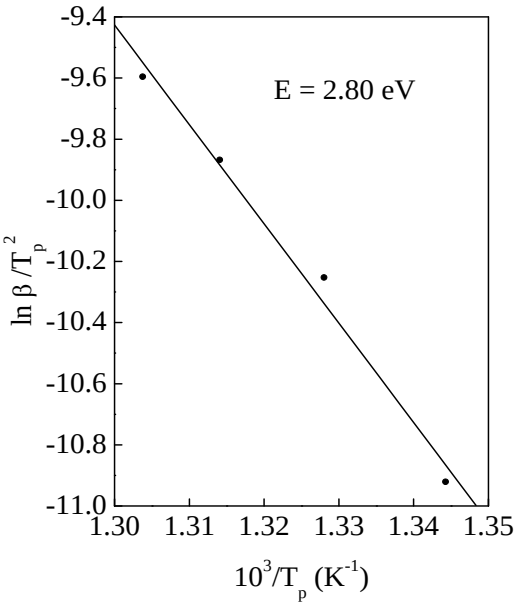

Fig.2. Kissinger plot from the kinetic rate of DTA thermogram for the determination of activation energy of α-Fe(Si) phase of $Fe_{73.5}Cu_1Mo_{1.5}V_{1.5}Si_{13.5}B_9$ alloy.

Activation energy of crystallization obtained in this study is comparable to our previous results [8] [9].

$Fe_{73.5}Cu_1Mo_{1.5}V_{1.5}Si_{13.5}B_9$ nanocrystalline ribbon is similar to Finemet type of alloys exhibiting ultra-soft magnetic properties. However, the appearance of the best properties is sensitive to the alloys' annealing temperature and time.

These nanocrystalline amorphous ribbons were prepared by rapid quenching technique and the amorphous state was confirmed by x-ray diffraction method.

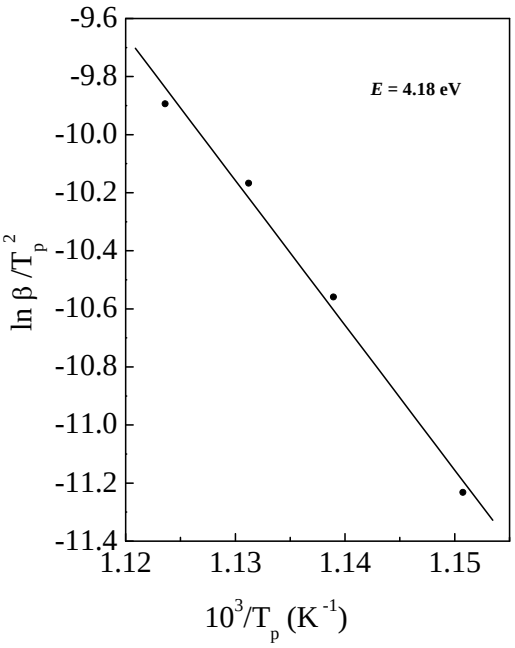

Fig.3. Kissinger plot from the kinetic rate of DTA thermo gram for the determination of activation energy of Fe-B phase of $Fe_{73.5}Cu_1Mo_{1.5}V_{1.5}Si_{13.5}B_9$ alloy.

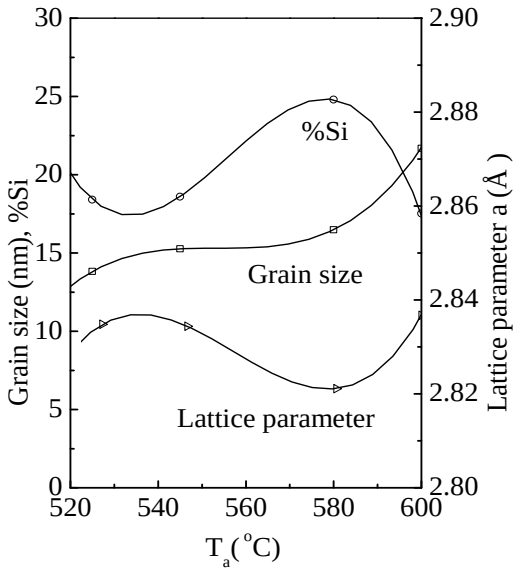

Fig.4. Variation of lattice parameter, silicon content at % and grain size of α-Fe(Si) with annealing temperature.

In Figure 4, X-ray diffraction spectra of as-cast and annealed samples at different annealing temperatures for annealing time 30 minutes have been presented. In the as-cast condition the sample is in the amorphous state having broad diffused pattern characteristic of crystalline phase since no crystalline phase have formed due to rapid quenching. When the sample is annealed above the crystallization temperature nanocrystalline grain of α-Fe(Si) is formed from amorphous precursor. For the samples annealed at or above 525°C, peaks corresponding to crystalline phases appear, which have been identified as bcc □-Fe(Si) solid solution produced in the amorphous matrix. With the increase of annealing temperature the peaks become narrower with higher intensity indicating that the crystalline volume fraction has increased. The other metalloid element B is practically insoluble in α-Fe(Si), whose solubility is less than 0.01% [10].

In Figure 5, the lattice parameter (a_o), grain size (D) and Si content of □-Fe(Si) nanograins dispersed in the surrounding amorphous matrix have been presented for various annealed samples in the temperature range between 525°C and 600°C. With the increase of annealing temperature lattice parameter decreases until 580°C beyond which it starts increasing. The lattice parameter of□ □-Fe(Si) phases are always smaller than that of pure Fe, the value of which is 2.866 Å.

Thus it can be assumed that the decrease of lattice parameter is due to the contraction of □-Fe lattice as a result of diffusion of the silicon with smaller atomic size into the iron lattice with larger atomic size forming a substitutional solid solution during the crystallization process to form □-Fe(Si).

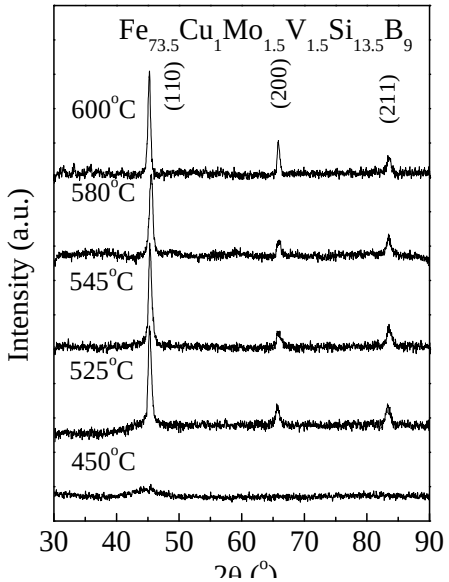

Fig.5. X-ray diffraction pattern of (a) as-cast and samples annealed at (b) T_a = 525°C, (c) T_a=545°C, (d) T_a= 580°C and (e) T_a = 600°C for $Fe_{73.5}Cu_1Mo_{1.5}V_{1.5}Si_{13.5}B_9$.

From the established quantitative relationship between lattice parameter and Si content of Fe-Si alloys [11], Si contents of □-Fe(Si) nanograins have been determined and shown in Figure 5. The Si content of □-Fe(Si) increases with the increase of annealing temperature attaining a maximum value of about 24 at.% at 580°C beyond which it starts decreasing. When the samples are annealed above 580°C, an increase of lattice parameter with subsequent decrease of Si content indicates that at higher annealing temperature some of the silicon diffuses out of the □-Fe(Si) nanograins.

International Journal of Engineering Innovation & Research
Volume 4, Issue 5, ISSN: 2277 – 5668

In Figure 5, the mean grain size of the nanograins determined from the x-ray fundamental peak (110) of the bcc α-Fe(Si) using the Scherrer's formula $D = 0.9\lambda/\beta\cos\theta$ [12] has been presented. Here, λ is the wave-length of Cu-K_α radiation and β is the full width half maximum (FWHM).

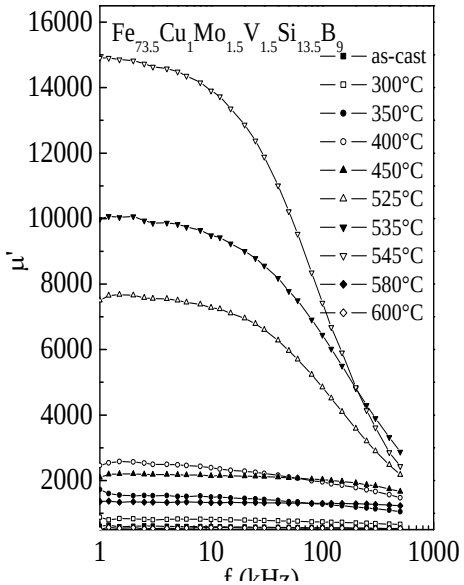

Fig.6. Frequency dependence of initial permeability μ' for $Fe_{73.5}Cu_1Mo_{1.5}V_{1.5}Si_{13.5}B_9$ alloy at different annealing temperatures T_a.

The grain size increases gradually up to 580°C and attains a limiting value of about 16 nm. An abrupt increase of grain size above 580°C is noticed attaining a value of about 22 nm. The formation of grain size in the nanometer regime can be ascribed to the combined addition of Cu, Mo and V in this composition.

In order to correlate the microstructural features with soft magnetic properties of the alloys under study, magnetic initial permeability of the toroidal shaped samples annealed at different temperatures are measured in very low field. The magnetic properties of the soft magnetic materials are mainly determined by the domain wall mobility especially in the range of reversible magnetization.

Figure 6 shows the real part of the complex initial permeability μ' as a function of frequency in the range 1 to 500 kHz for the as-cast and annealed samples at different temperatures of 300°C to 600°C for 30 minutes holding time. The general characteristic of the curve is that μ' remains fairly constant up to some critical frequency and then drops rapidly due to the increase of the loss component of the complex permeability. The low frequency value of μ' generally increases with the increase of annealing temperature while the critical frequency decreases. The frequency at which the real part of the complex initial permeability μ' drops is called resonance frequency. It is seen from the figure that the initial permeability μ' for the as-cast sample is very low.

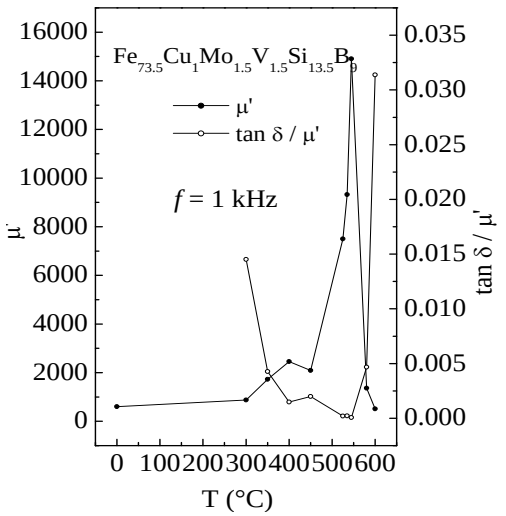

Fig.7. Variation of initial permeability μ' and relative loss factor $\tan\delta/\mu'$ for $Fe_{73.5}Cu_1Mo_{1.5}V_{1.5}Si_{13.5}B_9$ alloy at fixed frequency f=1kHz with annealing temperature T_a.

The initial permeability, μ' at the frequency of 1 kHz generally increases with the increase of annealing temperature. This trend of increase of low frequency permeability upon annealing temperature is observed up to T_a = 545°C. An increase of initial permeability upon annealing temperature was observed due to irreversible structural relaxation of the amorphous matrix, i.e. stress relief and also increase of the packing density of atoms by removing micro-voids through the annealing process and hence changing the degree of chemical disorder [13].

For the annealing temperature of 580°C the low frequency permeability decreases sharply. A sharp fall of initial permeability is noticed for the sample annealed at T_a = 600°C. The decrease of initial permeability is due to the formation of Fe-B phase in the amorphous matrix. This figure also shows that the resonance frequency decreases with the increase of annealing temperature up to 545°C.

The high permeability ribbons can be used as core materials only in a limited frequency range.

The role of amorphous phase in intergrain coupling can be understood well from the annealing temperature dependence of initial permeability and relative loss factor. Initial permeability μ' and relative loss factor $\frac{\tan\delta}{\mu'}$ measured at room temperature has been presented as a function of annealing temperature T_a at a fixed frequency of 1 kHz and presented in Figure 7. The curve reveals itself strong dependence of initial permeability upon annealing temperature. When annealed at temperature below the onset of crystallization, i.e. up to 450°C, an increase of initial permeability with annealing temperature was observed due to irreversible structural relaxation of the amorphous matrix, i.e. stress relief, increase of packing density by annealing out micro-voids and changing the degree of chemical disorder. Further increase of annealing temperature in the range of 450° to 545°C leads to a sharp increase of permeability due to crystallization of α-Fe(Si)

phase and increased volume fraction of nanograins coupled via exchange interaction resulting in a reduction of anisotropy energy. An enhancement of initial permeability by two orders of magnitude was observed for the annealing temperature of 545°C, where the maximum value of μ′ has reached upto the value of 14905. On the other hand it is seen from Figure 7 that as the annealing temperature is increased, relative loss factor $\frac{\tan\delta}{\mu'}$ drops sharply, reaches a minimum value ($\frac{\tan\delta}{\mu'} = 7.02\times10^{-5}$) when the annealing temperature is 545°C. Beyond this temperature μ' drops to lower value drastically and $\frac{\tan\delta}{\mu'}$ increases. The probable reason might be the evolution of boride phase, which leads to the increase of anisotropy to a high value that essentially reduces the local exchange correlation length weakening the intergranular magnetic coupling as a result of which magnetic hardening takes place.

Field dependence of magnetization has been measured and presented for samples annealed at different temperature which has been presented in Figure 8. It can be observed from Figure 8 that the magnetization has reached to saturation value at low field characterizing the soft magnetic properties of the materials. Saturation magnetization M_s, increases up to 400°C and then decreases. The increase in M_s can be attributed to the irreversible structural relaxation and varying degree of chemical disorder. The decrease in M_s corresponds to the optimum nanocrystallized state with high volume fraction of α-Fe(Si) nanograins. This may be interpreted as due to the enrichment of nanograins with Si by diffusion resulting in a decrease of magnetic moment of Fe and enrichment of the residual amorphous phase with Mo and V.

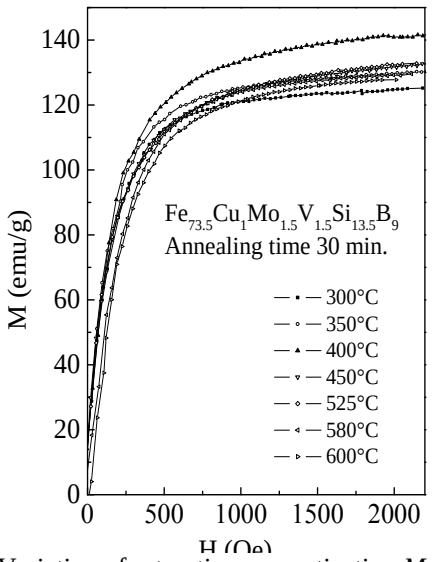

Fig.8. Variation of saturation magnetization M_s with applied magnetic field H for sample annealed at different temperatures.

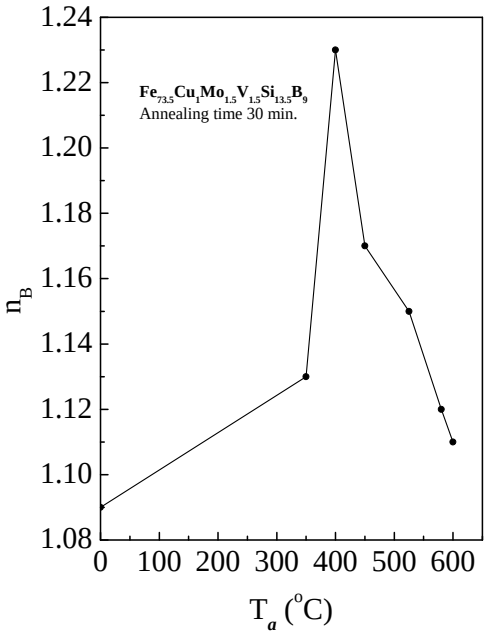

Fig.9. Effect of annealing temperature, $T_a$on Bohr magneton per molecule n_B.

Annealing temperature dependence of Bohr magneton n_B at room temperature is presented in Figure 9. The Bohr magneton is determined by $n_B = \frac{M_s \times \text{Mol.Wt.}}{N \times \mu_B}$, where n_B, Bohr magneton per molecule; M_s, saturation magnetization (in emu/gm); N, Avogadro's number and μ_B, Bohr magneton in erg/gauss. From Figure 8 and 9 it has been observed that both M_s and n_B increases in the amorphous relaxed state while in noncrystalline state, M_s and n_B decreases.

Amorphous alloys are basically metastable materials. Hence structural relaxation can occur even though the alloy remains amorphous when they are annealed at temperature well below the crystallization temperature. The increase in M_s can be attributed to the irreversible structural relaxation and varying degree of chemical disorder. The decrease in M_s corresponds to the optimum nanocrystallized state with high volume fraction of α-Fe(Si) nanograins. This may be interpreted as due to the enrichment of nanograins with Si by diffusion resulting in a decrease of magnetic moment of Fe and enrichment of the residual amorphous phase with Mo and V.

IV. Conclusion

Nanocrystalline structures offer an interesting opportunity for tailoring good soft magnetic properties. There is much scope for future research on this nanocrystalline material. Controlling the magnetic characteristics by choosing appropriate alloy composition is needed. To determine the best soft magnetic properties, selection of the annealing temperature and duration of the heat treatment are therefore essential. Transmission electron microscopy observation of growing crystallites

for microstructure study and measurements of coercivity, magnetic anisotropy and magnetostriction for this material are proposed research work for the future.

REFERENCES

[1] Yoshizawa, Y. and Yamauchi, K. Mater. Trans. JIM. 31 (1990) 307-314.
[2] Noh, T. H., Lee, M. B., Kim, H. J. and Kang, I. K., J. Appl. Phys. Vol. 67 (1990) 5568-5570.
[3] Kataoka, N., Matsunaga, T., Inoue, A., and Masumoto, T., Mater. Trans. JIM 30 (1989) 947-950.
[4] Yoshizawa, Y. and Yamauchi, K., IEEE. Trans. J. Magn. 5 (1990) 1070-1076.
[5] Müller, M. and Mattern, N., J.Mag.Mag.Mater.Vol.136 (1994) 79-87.
[6] Herzer, G., Nanocrystalline Soft Magnetic Alloys, in: Buchow K. H. J. (Ed.) Handbook of Magnetic Materials, Elsevier Science B. V. North Holland, (1997), Vol. 10, pp. 415-462.
[7] Suzuki, K., Makino, A., Kataoka, N., Inoue, A. and Masumoto, T., J. Appl. Phys. 70 (1991) 6232-6237.
[8] Hakim, M. A. and Hoque, S. M., J. Magn. Magn. Mat. 284 (2004) 395-402.
[9] Hoque, S. M., Hakim, M. A., Khan, F. A. and Chau, N., Mater. Chem. and Phys. 101 (2007) 112-117.
[10] Kubaschewski, O., Iron Binary Phase Diagrams, Springer-Verlag, Berlin, Heidelberg New York Verlag Stahleisenm. b.H. Düsseldorf, 1982.
[11] Bozorth, R. M., Frromagnetism, D. Van. Nostrand Company. Inc. Princeton, New Jersey, 1964.
[12] Cullity, B. D., Elements of X-ray Diffraction, Addison-Wesley, London, 1959.
[13] Lachowic, H. K. and Ślawska-Waniewska, A., J. Mag. Mag. Matter. 133 (1994) 238-242.

AUTHOR'S PROFILE

S. M. Abdur Rahim,
Assistant Professor, Department of Applied Physics, Electronics and Communication Engineering, Islamic University, Kushtia, Bangladesh,
Email: smrahimiu@yahoo.com; smrahim@aece.iu.ac.bd
Cell: +8801715-544555

Dr. Sheikh Manjura Hoque
Head and Principal Scientific Officer, Materials Science Division, Atomic Energy Centre-4, Kazi Nazrul Islam Avenue, P.O. Box-164, Ramna, Dhaka-1000, Bangladesh.
Phone: +88-02-8626603, Fax: +88-2-8617946

Dr. Md. Manjurul Haque
Professor, Department of Applied Physics Electronics and Communication Engineering, Islamic University, Kushtia, Bangladesh.
E-mail : manju_iu@yahoo.com; manjurulkst@gmail.com
Mobile: +88-01715157526

S. Akhter
Director, Atomic Energy Centre, Kazi Nazrul Islam Avenue, P.O. Box-164, Ramna, Dhaka-1000, Bangladesh, Phone: +88-02-9675367, Fax: +88-2-8617946